When the unheated mineral grains were examined with XRD, none of these peaks could be conclusively identified. Therefore, the remaining unheated portion of the sample showing the stishovite NMR peak was subjected to further acid treatment on a steambath. The sample was first digested 24 hours in 1:1 HNO_3, followed by 24 hours in 1:1 HCl and a small amount of solid ethylenediaminetetraacetic acid, which reduces precipitation of unwanted calcium and magnesium fluorides during HF treatment. Residual granules were twice partially digested in 1:1 HF in an open platinum dish and dried on a steambath. An XRD pattern of these final insoluble grains indicated the presence of quartz, rutile, anatase, and zircon. Furthermore, eight clearly observed XRD peaks (Fig. 2) have the *d*-spacings of stishovite (Table 2).

The combination of both ^{29}Si MAS NMR and XRD data demonstrate that stishovite occurs in the K-T boundary layer at Raton, New Mexico. Both NMR and powder XRD are bulk analytical techniques; neither method can determine precise size nor location of phases in a sample. However, two potential stishovite precursor materials, zircon and quartz, occur in the boundary layer at Raton and in K-T boundary deposits at Clear Creek North, Colorado (*19*). Transmission electron microscope studies of Clear Creek quartz grains have shown that shock lamellae contain glassy material that, unlike natural heat-fused silica (lechatelierite), appears to be slightly denser than surrounding host quartz (*19*). At the Ries impact structure in Germany, stishovite has been reported in diaplectic (glassy) quartz shock lamellae (*20*). If stishovite in the Raton K-T boundary layer is formed from quartz rather than zircon, it may occur in these dense glassy lamellae.

Comparison with other ^{29}Si-MAS NMR spectra obtained in our laboratory suggests that the K-T boundary grains in the NMR split contained 1 to 3 mg of stishovite. Therefore, we estimate that from 16 to 48 mg of stishovite was in the 8 g of material separated from the original 8 kg sample. We were unable to determine the proportion of stishovite to other mineral phases in the K-T boundary sample. Stishovite, because of its short relaxation time, can be detected with enhanced sensitivity relative to other mineral phases (*10, 12*). The long recycle delays needed for more quantitative measurements would seriously degrade the sensitivity to stishovite.

At known impact structures, coesite commonly occurs in the same rocks as stishovite (*8, 20*). However, coesite cannot always be observed in samples from these sites, even where stishovite is present at concentrations greater than 0.5% relative to primary quartz. Coesite was also not observed in stishovite-bearing samples from laboratory shock experiments (*21*). During our study, three similar samples (about 8 kg each) of boundary material were processed and examined. Coesite could not be detected, and stishovite was observed in all splits from only one sample. Our results indicate that stishovite is unevenly distributed within K-T boundary deposits and occurs in very small amounts. Even when found in situ at thoroughly studied impact structures, silica pressure polymorphs are rare and occurrences are sporadic. Detection of stishovite is strong evidence that shocked components in K-T boundary sediments result from extraterrestrial impact: it is thermally unstable at moderate pressures and should not survive the prolonged heat of a near surface volcanic event.

REFERENCES AND NOTES

1. L. W. Alvarez, W. Alvarez, F. Asaro, H. V. Michel, *Science* **208**, 1095 (1980).
2. B. F. Bohor *et al.*, *ibid.* **224**, 867 (1984).
3. B. F. Bohor *et al.*, *ibid.* **236**, 705 (1987).
4. A. Hallam, *ibid.* **238**, 1237 (1987).
5. S. M. Stishov and S. V. Popova, *Geochemistry* **10**, 923 (1961).
6. K. Kusaba, Y. Syono, M. Kikuchi, K. Fukuoka, *Earth Planet. Sci. Lett.* **72**, 443 (1985).
7. B. J. Skinner and J. J. Fahey, *J. Geophys. Res.* **68**, 5595 (1963).
8. S. W. Kieffer, *ibid.* **76**, 5449 (1971); ———, P. P. Phakey, J. M. Christie, *Contrib. Mineral. Petrol.* **59**, 41 (1976).
9. J. J. Fahey, *Am. Mineral.* **49**, 1643 (1964).
10. J. V. Smith and S. C. Blackwell, *Nature* **303**, 223 (1983); J. M. Thomas, J. M. Gonzalez-Calbert, C. A. Fyfe, G. C. Gobbi, M. Nicol, *Geophys. Res. Lett.* **10**, 91 (1983).
11. K. A. Smith, R. J. Kirkpatrick, E. Oldfield, D. M. Henderson, *Am. Mineral.* **68**, 1206 (1983); G. Engelhardt and D. Michel, *High-Resolution Solid-State NMR of Silicates and Zeolites* (Wiley and Sons, New York, 1987); R. Dupree, D. Holland, M. G. Mortuza, *Nature* **328**, 416 (1987).
12. W.-H. Yang *et al.*, *Meteoritics* **21**, 117 (1986).
13. J. McHone and R. A. Nieman, *ibid.* **23**, 289 (1988).
14. C. L. Pillmore and R. M. Flores, *Geol. Soc. Am. Spec. Pap. 209* (1987). Stratigraphy described in detail for site located at latitude 36°54′12″N, longitude 104°27′04″W.
15. Frantz settings: 10° down-slope, 5° tilt (magnetic up), 1.5 ampere current.
16. Spectra were obtained with a Bruker AM-400 spectrometer equipped with a multinuclear MAS probe operating at 79.5 MHz for ^{29}Si. Samples (450–500 mg) were spun at 4.5 to 5.2 KHz in single air-bearing Delrin rotors. The magic angle was adjusted by maximizing spinning side-bands of the ^{79}Br resonance in KBr, and chemical shifts were referenced to external TMS and are reproducible to about ±0.3 ppm. Magnetic field drift was compensated to better than 0.5 ppm per day. Free induction decays (15,000 to 60,000) were acquired over a period of 1 to 3 days for a spectral width of 35,714 Hz, an acquisition time of 115 ms, a 75° pulse width, and a delay of 5 s between acquisitions.
17. B. L. Sherriff and J. S. Hartman, *Can. Mineral.* **23**, 205 (1985).
18. E. C. T. Chao, J. J. Fahey, J. Littler, D. J. Milton, *J. Geophys. Res.* **67**, 419 (1962).
19. A. Gratz *et al.*, *Lunar Planet. Sci. XIX*, 419 (1988).
20. D. Stoffler, *J. Geophys. Res.* **76**, 5474 (1971).
21. P. S. De Carli and D. J. Milton, *Science* **147**, 144 (1965).

22. The work of J.F.M. was partially supported by R. S. Dietz and Barringer Crater Company, Princeton, New Jersey. We thank T. I. Emilsson and C. L. Pillmore for helpful discussions. Samples were collected with the assistance of M. R. Owen. The NMR spectrometer was purchased with assistance from Arizona State University and National Science Foundation grant CHE-8409644.

11 November 1988; accepted 19 January 1989

Sequence-Specific Peptide Cleavage Catalyzed by an Antibody

BRENT L. IVERSON AND RICHARD A. LERNER

Monoclonal antibodies have been induced that are capable of catalyzing specific hydrolysis of the Gly-Phe bond of peptide substrates at neutral *p*H with a metal complex cofactor. The antibodies were produced by immunizing with a Co(III) triethylenetetramine (trien)–peptide hapten. These antibodies as a group are capable of binding trien complexes of not only Co(III) but also of numerous other metals. Six peptides were examined as possible substrates with the antibodies and various metal complexes. Two of these peptides were cleaved by several of the antibodies. One antibody was studied in detail, and cleavage was observed for the substrates with the trien complexes of Zn(II), Ga(III), Fe(III), In(III), Cu(II), Ni(II), Lu(III), Mg(II), or Mn(II) as cofactors. A turnover number of 6×10^{-4} per second was observed for these substrates. These results demonstrate the feasibility of the use of cofactor-assisted catalysis in an antibody binding site to accomplish difficult chemical transformations.

MONOCLONAL ANTIBODIES HAVE been elicited that can catalyze a number of chemical reactions, including ester (*1*) or carbonate (*2*) hydrolysis, a stereospecific lactonization reaction (*3*), bimolecular amide formation (*4*), a stereospecific Claisen rearrangement (*5*), hydrolysis of a *p*-nitroanilide amide (*6*), and a photochemical cleavage of thymine dimers

Department of Molecular Biology, The Research Institute of Scripps Clinic, La Jolla, CA 92037.

(7). Recently, a system was reported in which a reactive group was covalently attached to an antibody binding pocket (*8*).

Most of these catalytic antibodies have been produced by immunizing an animal with a "transition-state analog" compound that, in both shape and charge distribution, resembles a high-energy structure thought to be an intermediate in the reaction pathway. The antibodies then catalyzed the desired reaction, presumably through binding forces that lower the energy of the intermediate and thus reduce the overall reaction barrier (*1–5*). In some instances, chemically reactive amino acid side chains in the antibody binding pocket have been implicated in the catalyzed reaction (*6, 7, 9*). We have investigated a new approach whereby a chemical cofactor (a metal complex) is noncovalently bound by the antibody together with the substrate in order to provide chemical reactivity in the antibody binding pocket. In this way it was anticipated that a reaction, even one as energetically demanding as peptide hydrolysis, could be mediated by an antibody.

We report the production and initial characterization of monoclonal antibodies that catalyze the site-specific hydrolysis of a Gly-Phe peptide bond at *p*H 6.5 with various metal cofactors. The recently reported rate of 3×10^{-9} s^{-1} for the uncatalyzed hydrolysis of a peptide, corresponding to a half-life of approximately 7 years, puts the difficulty of this reaction into perspective (*10*).

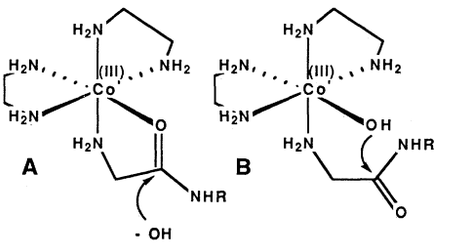

Scheme 1. Metal-amide interactions.

Metal-ion participation in amide bond hydrolysis has been observed in both enzymatic (*11, 12*) and model systems (*13–16*), and at least two types of interactions between metal and amide have been identified. In the first type (reaction A in Scheme 1), the metal atom directly coordinates the amide carbonyl oxygen. The resulting polarization of the carbonyl group facilitates nucleophilic attack of hydroxide or water at the carbonyl carbon atom. Another mode of catalysis consists of the delivery of a metal-bound hydroxide to the carbonyl carbon atom of the amide (reaction B in Scheme 1). In the case of the stoichiometric Co(III)-promoted amide hydrolysis in aqueous solution in the *p*H range 9 to 14, both types of interaction increased the rate of amide hydrolysis significantly; however, the second type involving the metal-bound hydroxide nucleophile was much more efficient (*14*). For the Zn(II)-containing protease enzymes thermolysin and carboxypeptidase A, it is possible that one or both types of interaction are operating to increase the rate of amide hydrolysis (*12, 17*). We reasoned that if antibodies could be produced that simultaneously bind a metal cofactor and a peptide substrate in the appropriate geometry, the hydrolysis of the peptide in the antibody binding pocket would be facilitated. Furthermore, the specificity of binding so characteristic of antibody-antigen interactions should provide these proposed proteolytic antibodies with readily programmable sets of selective sequence specificities.

In order to induce proteolytic antibodies, the hapten **1** used for immunization consisted of a relatively kinetically inert Co(III) (trien) moiety complexed to the secondary amino acid site of a four-residue peptide (see Fig. 1) (*18*). We chose β-Ala-Gly (where β-Ala is β-amino alanine) as the carboxyl-terminal residues as they would form a flexible linker between the hapten and the carrier protein. Since a kinetically inert metal would probably not substitute ligands quickly enough to be an ideal hydrolysis cofactor (*19*), it was hoped that some of the monoclonal antibodies to **1** would have a somewhat promiscuous binding pocket capable of accommodating trien complexes

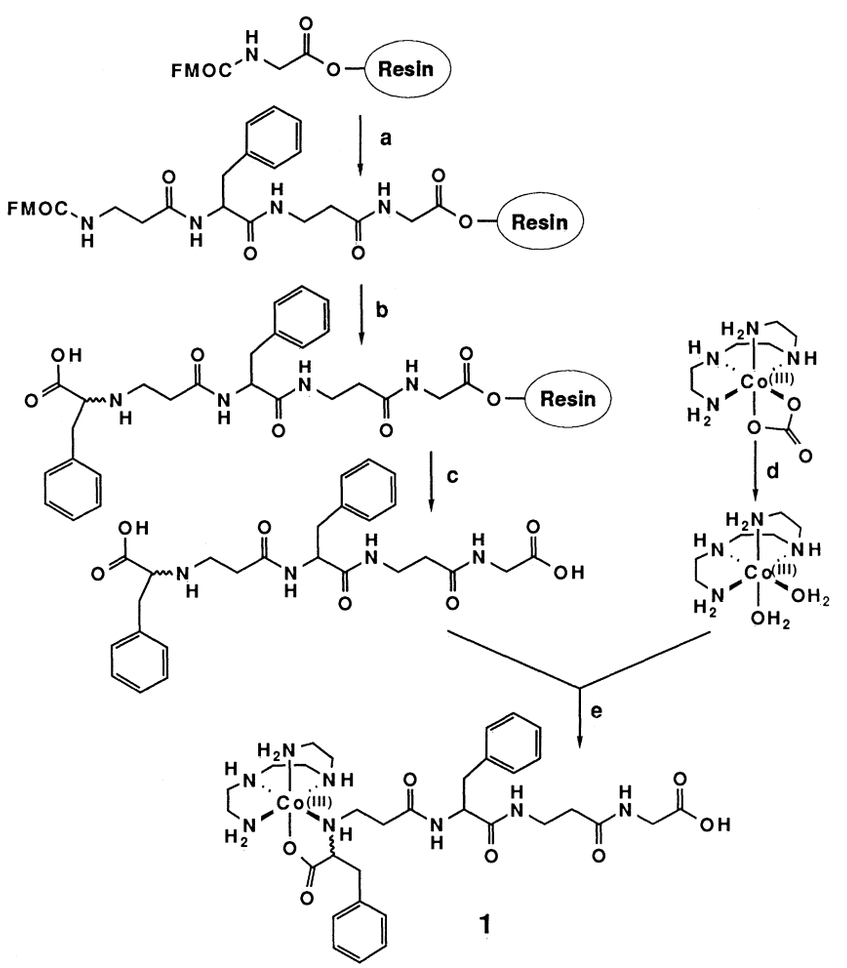

Fig. 1. Synthetic scheme for the production of hapten **1**. The solid-phase portion of the synthesis was carried out with the peptide linked to SASRIN resin (Bachem Biosciences Inc.). In reaction a, a standard solid-phase protocol was followed with the use of fluorenyl methoxycarbonyl (FMOC) amino acids (*18*). Reaction b was performed with 2 equivalents 3-phenylpyruvate, 2.5 equivalents $NaBH_3CN$, in 4:1 tetrahydrofuran (THF): H_2O *p*H 7.5. The reaction was carried out directly in the shaker apparatus, and after 12 hours the reaction was judged complete by ninhydrin. In reaction c, we used 1% trifluoroacetic acid in dichloromethane. The peptide was purified by preparative reversed-phase chromatography. In reaction d, 1.2 equivalents HCl in H_2O were used. In reaction e, 1.1 equivalents of peptide in H_2O, *p*H 8.5, were heated at 65°C for 6 hours (*13*). The metal complex **1** was purified by ion-exchange chromatography on CM-50-120 Sephadex eluted with 0.2*M* KCl. The appropriate fraction was lyophilized to dryness, and the pure product was taken up in cold ethanol. Hapten **1** was covalently attached to the carrier protein with 100 m*M* 1-ethyl-3-(3-dimethylaminopropyl)carbodiimide (EDC), 5 m*M* *N*-hydroxysulfosuccinimide (sulfo-NHS), *p*H 7.5.

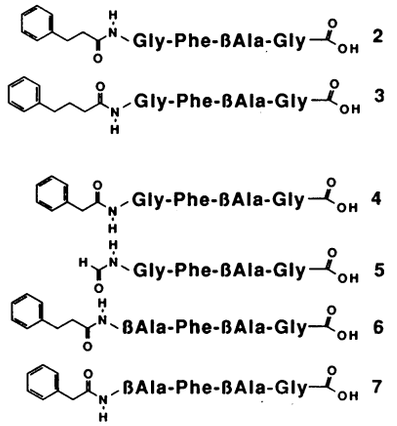

Fig. 2. Structures of the synthetic peptides tested as possible proteolytic antibody substrates. Compounds **2** and **3** were cleaved by several of the proteolytic antibodies, whereas compounds **4** through **7** were not substrates.

of not only Co(III) but also kinetically labile metals such as Zn(II) or Fe(III), which should be hydrolytically active cofactors. In an earlier study, antibodies generated against an EDTA-type complex of In(III) were shown to bind several different EDTA-metal complexes (*20*). Thus the general strategy is to immunize with a kinetically inert coordination complex in order to induce a binding pocket that could accept a kinetically labile complex of similar geometry.

The binding pockets of proteolytic antibodies derived from hapten **1** were intended to bring the metal complex and the peptide together in an appropriate geometry (*21*) in order to allow and possibly facilitate the metal-catalyzed peptide hydrolysis reaction and, finally, to release the products. In this regard, hapten **1** differs from a true transition-state analog in that no portion of the molecule exactly resembles the presumed metal-bound tetrahedral intermediate. The molecule was designed more as a template around which a complementary proteolytic antibody binding site would be produced that would be capable of simultaneously binding an octahedral metal cofactor complex and the substrate peptide. Depending on the conformation of hapten and substrate, it was anticipated that the proteolytic antibody binding pocket would accommodate the scissile bond of a substrate in an orientation that would place the carbonyl group near the metal atom of a simultaneously bound metal trien complex. The metal complex could then facilitate amide bond hydrolysis by binding and polarizing the carbonyl group, by promoting the nucleophilic attack of a metal bound hydroxide species, or by both processes operating together. Either pathway, or a combination of the two, would lead to a metal-bound tetrahedral intermediate. Breakdown of this metal-bound tetrahedral intermediate, protonation of the leaving amine function, and release of the products would complete the hydrolysis reaction.

Hapten **1** was covalently attached to keyhole limpet hemocyanin, and 129GIX$^+$ mice were immunized with the resulting conjugate in a standard immunization regimen (*9*). One half of the spleen from the highest responding mouse was used for fusion with SP2/0 myeloma cells (*6*). A total of 13 hybridomas were identified and maintained that secreted monoclonal antibodies capable of specifically binding hapten **1** as determined by an enzyme-linked immunosorbent assay (ELISA).

Competition ELISA studies (*22*) indicated that the 13 antibodies could accommodate a variety of trien metal complexes in their binding sites, and subtle differences in metal binding specificities between different antibodies were observed. In general, Cd(II)(trien), Co(III)(trien), Cu(II)(trien), Fe(III)(trien), Ni(II)(trien), Pd(II)(trien), and Zn(II)(trien) were bound with the highest affinity, although binding to metal complexes such as Co(II)(trien), Ga(III)(trien), In(III)(trien), La(III)(trien), Lu(III)(trien), Mg(II)(trien), Mn(II)(trien), Sc(III)(trien), Tb(III)(trien), and Yb(III)(trien) could also be detected with some of the antibodies. Negligible amounts of competition was observed when only metal salt was added (no trien ligand).

Each of the 13 monoclonal antibodies were screened for proteolytic activity with the six substrate peptides **2** through **7**. Several different trien metal complexes were used as possible cofactors. A rapid and sensitive peptide cleavage assay was developed that detected the free amine groups revealed during any amide hydrolysis of the substrates. The assay involved spotting the reaction mixture on a silica thin-layer chromatography (TLC) plate, which was then eluted with a 1:4 water:methanol solvent mixture. Any hydrolyzed peptide product eluted near the solvent front, whereas proteolytic antibody, trien alone, and metal-trien cofactor remained at the origin. After elution, the plate was sprayed with an acetone solution of fluorescamine, and any fluorescent green material (long-wavelength UV) near the solvent front indicated substrate hydrolysis. As little as 2 μ*M* of product amine could be detected with this procedure. The routine nature of the assay facilitated investigation of a large number of reaction parameters with each proteolytic antibody.

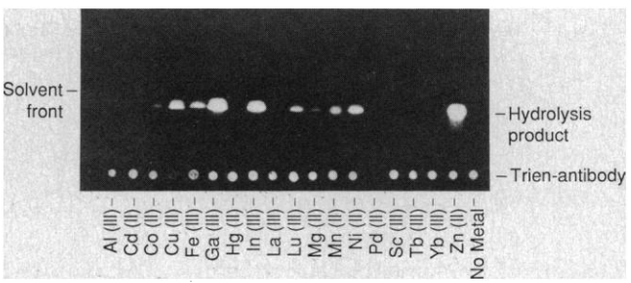

Fig. 3. Cleavage of substrate **2** catalyzed by 28F11 in the presence of various 1:1 trien-metal complexes. In each reaction, 10 μ*M* 28F11, 1.2 m*M* **2**, and 3 m*M* trien-metal complex were placed in 50 m*M* NaCl, 75 m*M* phosphate buffer, *p*H 6.5. The last lane is a control in which an otherwise normal reaction is run with **2**, trien, and antibody, but with no metal cofactor. All of these reactions were incubated at 37°C for 5 days, 3.5 μl of each reaction was spotted on a silica TLC plate, which was eluted with 4:1 methanol:water. The plate was sprayed with a 0.2% fluorescamine solution in acetone and visualized with long-wavelength ultraviolet light. Cleavage product appears as the fluorescamine-reactive material eluting near the solvent front. Antibody and trien metal complexes remain at the origin. The trien reaction with the fluorescamine appears attenuated in the reactions containing the colored metals Co(II), Cu(II), and Pd(II). Before the reaction, the purified antibody was dialyzed against EDTA to remove metals, and all of the solutions were made with Chelex-treated, doubly distilled water. All of the metal salts used were of the highest purity currently available.

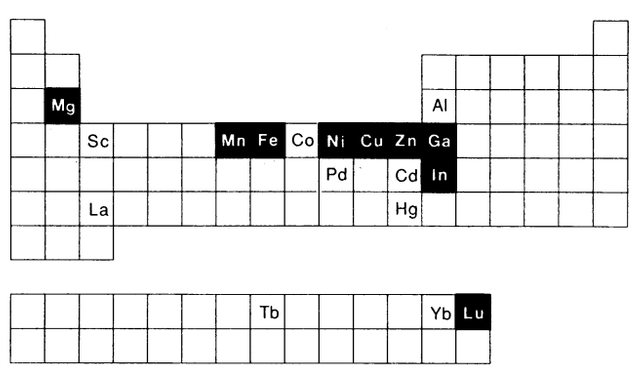

Fig. 4. Periodic table illustrating the locations of the metals tested for activity as cofactor in the hydrolysis of **2** catalyzed by 28F11. All of the metals were tested as the 1:1 trien-metal complex. Darkened boxes with white letters indicate active cofactors, whereas white boxes with black letters indicate metals that were tested but were found to be inactive as cofactors.

Several of the antibodies exhibited substantial cleavage of substrates **2** and **3** with various metal-complex cofactors (Fig. 2). The trien complexes of Zn(II), Fe(III), Ga(III), Cu(II), and Ni(II) were particularly effective cofactors. Peptides **4** through **7** were not substrates for any of the antibodies. One proteolytic antibody, 28F11, was selected and the peptide hydrolysis activity with substrate **2** was analyzed in detail.

In a typical reaction, 10 μM 28F11 was placed with 3 mM trien metal complex and 1.2 mM substrate peptide in 75 mM phosphate buffer. The reaction strictly requires the fully complemented system of proteolytic antibody, trien-metal, and substrate. Optimum cleavage was observed in the *p*H range 6.0 to 7.5 with most of the metals; however, different metals displayed different *p*H optima. As can be seen in Fig. 3, at *p*H 6.5, cleavage of **2** was observed with the trien metal complexes of (in decreasing relative order of activity) Zn(II), Ga(III), In-(III), Fe(III), Cu(II), Ni(II), Lu(III), Mn-(II), and Mg(II). Small but reproducible amounts of cleavage were observed with the trien complexes of Al(III) and Co(II). No cleavage by 28F11 was observed without cofactors when trien alone was used or with the trien complexes of Cd(II), Hg(II), La-(III), Pd(II), Sc(III), Tb(III), and Yb(III) (Fig. 4).

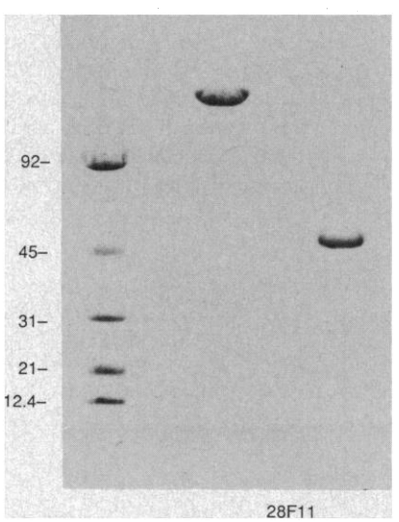

Fig. 5. SDS-polyacrylamide gel electrophoresis of purified IgG (middle lane) and Fab′ (right lane) of 28F11. Molecular-weight standards are shown in the left lane for comparison.

Zn(II)(trien) was observed to be the most efficient metal cofactor complex and exhibited its highest efficiency at a concentration of 1.5 mM. The Zn(II)(trien) reaction optimum was between *p*H 6.0 and 8.0 and at NaCl concentrations below 800 mM.

Several lines of evidence confirm that the proteolytic activity observed with 28F11 is due to a catalytic hydrolysis reaction taking place in the proteolytic antibody binding site that involves the Zn(II)(trien) as a noncovalently bound cofactor. First, the structures of substrates **2** and **3** resemble the structure of the peptide portion of hapten **1**. Second, highly purified Fab′ fragments produced by limited pepsin proteolysis (*6*) of 28F11 retained full catalytic activity (see Fig. 5). Third, the trien ligand was shown to be a requirement of the hydrolysis reaction, since Zn(II) alone exhibited only minimal activity (*23*). Finally, the reaction was effectively inhibited with hapten **1**.

The products of the reaction with **2** and **3** were isolated, and they were shown to be the result of specific cleavage between the Gly-Phe bond. The reaction of 3 mM Zn(II)(trien), 10 μM 28F11, and 4 mg of each substrate proceeded to completion in 8 days, which corresponds to 400 turnovers per antibody binding site and a turnover number of 6×10^{-4} s^{-1}. Only two fragments were observed from the reactions. These were isolated by preparative reversed-phase high-performance liquid chromatography (HPLC), and their structures were characterized by nuclear magnetic resonance (NMR). This analysis showed that the fragments could only have resulted from hydrolysis of the amide bond between the Gly and Phe residues of each substrate (Fig. 6).

A mechanistic interpretation of this proteolytic antibody-catalyzed peptide hydrolysis reaction probably depends upon a conformational analysis of hapten **1** or the substrates or both. Since the metal trien complex was shown to be a required cofactor, it is reasonable to assume the scissile bond of the substrate is directly coordinated to the metal at some point during the reaction. On first inspection, the Gly-Phe bond of the substrates **2** and **3** would seem to be somewhat removed from the metal binding site. Preliminary model-building studies have indicated that placing both phenyl rings adjacent to each other in **1** should indeed create a proteolytic antibody binding pocket in which **2** and **3** are bound in a geometry that places the scissile amide bond (Gly-Phe) adjacent to the metal binding site. The substrate specificity observed is consistent with this model, since substrates **4** through **7** are unlikely to adopt a similar geometry. A conformational analysis of compounds **1** through **7** is currently under way to help elucidate the details of this peptide hydrolysis reaction.

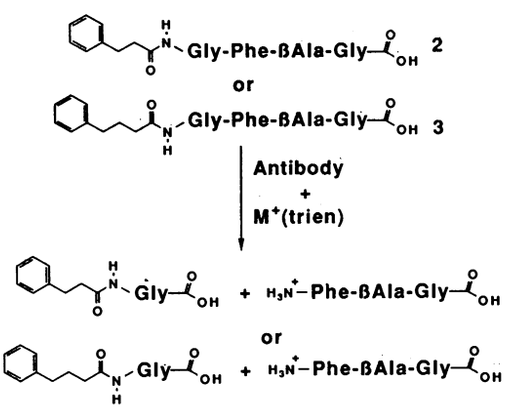

Fig. 6. Scheme of the peptide hydrolysis reactions catalyzed by 28F11 in the presence of trien-metal complexes. The identities of the products were confirmed by 300 MHz ^{1}H NMR analysis.

Peptide hydrolysis is but one example of a large number of reactions that could benefit from incorporation of a labile metal complex into an antibody binding site. The geometric constraints possible with these systems could be exploited to enforce stereoelectronic control on reactions such as aldol condensations or chiral epoxidations. Proteolytic antibodies have the potential to be the protein-cleaving equivalents of the restriction enzymes that cleave nucleic acids at specific sequences. We have demonstrated the feasibility of inducing proteolytic antibodies that can catalyze a sequence-specific peptide hydrolysis reaction. The challenge is to exploit the programmable nature of this technology and to develop novel proteolytic antibodies that catalyze the hydrolysis of other selected peptide or protein sequences.

REFERENCES AND NOTES

1. A. Tramontano, K. D. Janda, R. A. Lerner, *Science* **234**, 1566 (1986); A. Tramontano, A. A. Ammann, R. A. Lerner, *J. Am. Chem. Soc.* **110**, 2282 (1988).
2. S. J. Pollack, J. W. Jacobs, P. G. Schultz, *Science* **234**, 1570 (1986); J. Jacobs, P. G. Schultz, R. Sugasawara, M. Powell, *J. Am. Chem. Soc.* **109**, 2174 (1987).
3. A. D. Napper, S. J. Benkovic, A. Tramontano, R. A. Lerner, *Science* **237**, 1041 (1987).
4. S. J. Benkovic, A. D. Napper, R. A. Lerner, *Proc. Natl. Acad. Sci. U.S.A.* **85**, 5355 (1988); K. Janda, R. A. Lerner, A. Tramontano, *J. Am. Chem. Soc.* **110**, 4835 (1988).
5. D. Y. Jackson *et al.*, *J. Am. Chem. Soc.* **110**, 4841 (1988); D. Hilvert, S. H. Carpenter, K. D. Nared, M.-T. M. Auditor, *Proc. Natl. Acad. Sci. U.S.A.* **85**, 4953 (1988).
6. K. D. Janda, D. Schloeder, S. J. Benkovic, R. A. Lerner, *Science* **241**, 1188 (1988).
7. A. Cochran, R. Sugasawara, P. G. Schultz, *J. Am. Chem. Soc.* **110**, 7888 (1988).
8. S. J. Pollack, G. R. Nakayama, P. G. Schultz, *Science* **242**, 1038 (1988).

9. A. Tramontano, K. D. Janda, R. A. Lerner, *Proc. Natl. Acad. Sci. U.S.A.* **83**, 6736 (1986).
10. D. H. Kahne and W. C. Still, *J. Am. Chem. Soc.* **110**, 7529 (1988).
11. W. N. Lipscomb, *Acc. Chem. Res.* **15**, 232 (1982).
12. B. W. Mathews, *ibid.* **21**, 333 (1988).
13. J. P. Collman and D. A. Buckingham, *J. Am. Chem. Soc.* **85**, 3039 (1963).
14. D. A. Buckingham, D. M. Foster, A. M. Sargeson, *ibid.* **92**, 6151 (1970).
15. A. Schepartz and R. Breslow, *ibid.* **109**, 1814 (1987).
16. J. T. Groves and R. R. Chambers, *ibid.* **106**, 630 (1984).
17. D. W. Christianson and W. N. Lipscomb, *ibid.* **108**, 4998 (1988).
18. J. M. Stewart and J. D. Young, in *Solid Phase Peptide Synthesis* (Pierce Chemical, Rockford, IL, 1984), p. 82.
19. Co(III) complexes can cleave amide bonds, but the kinetically inert nature of the complexes results in stoichiometric rather than catalytic cleavage (*13–15*).
20. D. T. Rearden *et al.*, *Nature* **318**, 265 (1985).
21. The entropic component of enzymatic catalysis has been well discussed. See, for example, W. P. Jencks, in *Catalysis in Chemistry and Enzymology* (McGraw-Hill, New York, 1987), p. 64.
22. In these studies, the trien-metal complexes in solution were analyzed for their ability to inhibit antibody binding to hapten **1**. The hapten **1** was covalently attached to bovine serum albumin, which was itself noncovalently bound to the wall of the reaction vessel. Inhibition of binding to **1** was taken as evidence of specific binding of the trien-metal complexes in the antibody binding site.
23. The fact that any cleavage was observed at all without trien probably reflects the limited ability of the proteolytic antibody binding pocket to accommodate a Zn(II) aquo complex.
24. B.L.I. gratefully acknowledges a Junior Postdoctoral Fellowship from the California Division of the American Cancer Society. We thank our colleagues S. Benkovic, S. Brenner, S. Danishefsky, D. Hilvert, K. Janda, A. Tramontano, R. Ghadiri, and P. Wright for helpful discussions and criticisms. The authors also must acknowledge M. Mubaraki, D. S. Pasternak, and D. Schloeder for essential and superior technical assistance.

18 January 1989; accepted 27 January 1989

Sindbis Virus: An Efficient, Broad Host Range Vector for Gene Expression in Animal Cells

CHENG XIONG, ROBIN LEVIS, PING SHEN, SONDRA SCHLESINGER, CHARLES M. RICE, HENRY V. HUANG*

Sindbis virus, an enveloped virus with a single-stranded RNA genome, was engineered to express a bacterial protein, chloramphenicol acetyltransferase (CAT), in cultured insect, avian, and mammalian cells. The vectors were self-replicating and gene expression was efficient and rapid; up to 10^8 CAT polypeptides were produced per infected cell in 16 to 20 hours. CAT expression could be made temperature-sensitive by means of a derivative that incorporated a temperature-sensitive mutation in viral RNA synthesis. Vector genomic RNAs were packaged into infectious particles when Sindbis helper virus was used to supply virion structural proteins. The vector RNAs were stable to at least seven cycles of infection. The expression of CAT increased about 10^3-fold, despite a 10^{15}-fold dilution during the passaging. Sindbis virus vectors should prove useful for expressing large quantities of gene products in a variety of animal cells.

THE GENOME OF SINDBIS VIRUS, AN alphavirus, consists of a single-stranded RNA molecule that is 11703 nucleotides (nt) in length (*1, 2*). It is capped at the 5′ terminus and polyadenylated at the 3′ terminus. As the genomic RNA is infectious and serves as mRNA it is considered to have (+) polarity. The 5′ two-thirds of the genomic RNA is translated early during infection to produce the nonstructural proteins required for RNA replication and transcription; the 3′ end of the molecule encodes the structural proteins that are expressed at high levels throughout the infection cycle. Replication proceeds by the synthesis of a full-length (−) strand with the genomic RNA as template. The (−) strand then serves as template for the synthesis of new genomic RNA molecules. The three structural proteins are not translated from the genomic RNA, but are expressed via transcription of the (−) strand at an internal site, called the junction region, to produce a capped and polyadenylated subgenomic mRNA of 4100 nt that is colinear with the 3′-terminal one third of the genome. The subgenomic mRNA does not serve as a template for RNA synthesis nor is it packaged into mature virions. Translation of the subgenomic mRNA produces a polyprotein that is cleaved co- and posttranslationally by a combination of viral and host-encoded proteases to produce the capsid protein and the two envelope glycoproteins. The capsid protein complexes with the genomic RNA to form intracellular icosahedral nucleocapsids. These interact with the cytoplasmic domains of the transmembrane envelope proteins, resulting in the budding of virus at the plasma membrane.

Department of Microbiology and Immunology, Washington University School of Medicine, St. Louis, MO 63110.

*To whom correspondence should be addressed.

Three features of Sindbis virus suggest that it might be a useful vector for the expression of foreign genes. First, Sindbis virus has a wide host range; it is naturally transmitted by mosquitos to vertebrate hosts, usually a bird or a mammal (*3*). In the laboratory it infects cultured mammalian, avian, reptilian, amphibian, and some insect (mosquito and Drosophila) cells (*4*). Second, Sindbis virus gene expression occurs in the cytoplasm of the host cell, and is rapid and efficient. During the 8 to 12 hours of a typical infection at 37°C, some 10^7 to 10^8 molecules of viral structural proteins are synthesized by each infected cell. Thus a Sindbis virus vector might be useful for production of large amounts of gene products. Third, temperature-sensitive mutations in RNA synthesis are available (*5*) that may be used to modulate the expression of foreign genes by simply shifting cultures to the nonpermissive temperature at various times after infection.

As it is technically difficult to engineer RNA molecules, a cDNA clone of the Sindbis virus genome was placed immediately downstream of a promoter for phage SP6 DNA-dependent RNA polymerase, such that transcription in vitro with SP6 RNA polymerase produced infectious RNA transcripts (*6*). This approach has been used to map the cis-acting sequences required for replication and packaging of deletion-rear-

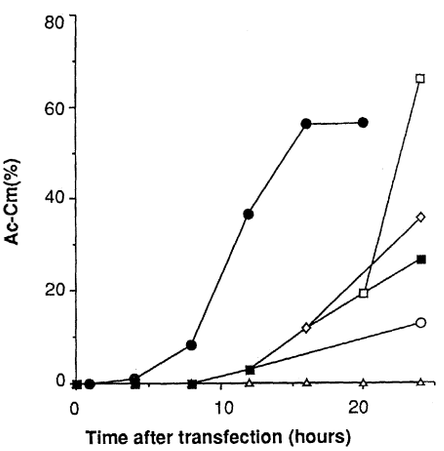

Fig. 1. Time course of CAT expression by TSCAT in chick embryo fibroblasts at 37°C, and by TSCAT-ts-6 at 30° with or without shifting to incubation at 40°C. The time course of CAT expression by TSCAT at 37° (●) in a representative experiment is shown. In an independent experiment parallel cultures were transfected with TSCAT-ts-6 at time 0. One set of cultures was maintained at 30° and sampled at the indicated times (■). At 0 or 8 (△), 12 (○), 16 (◇) and 20 (□) hours after transfection, plates from another set of cultures were shifted to and incubated at 40°C until 24 hours after transfection. Half of each cell extract was assayed for CAT activity, and the percent of chloramphenicol converted to acetylated chloramphenicol (Ac-Cm) is graphed.